ICHEP94 Ref. gls0229 c
Submitted to Pa 01
Pl 02

DELPHI 94-93 PHYS 410
1st June, 1994

New Measurement of the $\Gamma_{b\bar{b}}/\Gamma_{had}$ Branching Ratio of the Z with Minimal Model Dependence

Preliminary

DELPHI Collaboration

P. Billoir, H. Briand, V. Castillo, E. Cortina, E. Higón,
F. Martínez-Vidal, J. Salt and Ch. de la Vaissière

Abstract

A new measurement of $\Gamma_{b\bar{b}}/\Gamma_{had}$ branching ratio of the Z by double hemisphere tagging is presented. The basis of the method was already presented in a previous paper and now is applied to the data taken during 1992 at LEP in DELPHI. The tagging technique uses the precision tracking information given by the microvertex detector and it is based on a multivariate analysis technique. From about 440000 hadronic Z decays, $\Gamma_{b\bar{b}}/\Gamma_{had}$ is found to be

$$\Gamma_{b\bar{b}}/\Gamma_{had} = 0.2166 \pm 0.0058(stat) \pm 0.0031(syst) \pm 0.0005(\Gamma_{c\bar{c}}syst)$$

Combining this number with the obtained result for the 1991 data, a value of

$$\Gamma_{b\bar{b}}/\Gamma_{had} = 0.2196 \pm 0.0044(stat) \pm 0.0029(syst) \pm 0.0005(\Gamma_{c\bar{c}}syst)$$

is found. These results are almost independent of the modelling features.

1 Introduction

In the Standard Model, the decay $Z \to b\bar{b}$ differs from other hadronic Z decays because of the existence of final state electroweak interactions involving the *top* quark[1]. The effect of these vertex corrections can be isolated in the $\Gamma_{b\bar{b}}/\Gamma_{had}$ ratio, independently of other theoretical uncertainties in final state strong interactions or higher-order propagator terms, which cancel in the ratio. The value of $\Gamma_{b\bar{b}}/\Gamma_{had}$ can be used to infer the *top* mass through these vertex corrections [2] in the Minimal Standard Model. The prediction for the partial width ratio $\Gamma_{b\bar{b}}/\Gamma_{had}$ varies by over 3 % when m_t varies from 80 to 260 GeV/c^2, requiring a measurement at the level of 1 % precision to set meaningful constraints on the *top* quark mass. Moreover, the effect of these vertex corrections are sensitive to extensions of the Minimal Standard Model.

In this paper we present a new measurement of the $\Gamma_{b\bar{b}}/\Gamma_{had}$ branching ratio from about 440000 hadronic Z decays taken in 1992 with the DELPHI detector at LEP using the method already presented in [3] [4] for the 1991 data taken. The value $\Gamma_{b\bar{b}}/\Gamma_{had} = 0.2241 \pm 0.0063(stat) \pm 0.0044(syst) \pm 0.0012(\Gamma_{c\bar{c}} syst)$ was obtained. We have shown in that paper that it is possible, by combining two independent taggings applied to both hemispheres of the hadronic event, to measure the b flavour composition of a sample of hadronic events with a minimal model dependence. However, this needs a pure b sample in the limit of hard cuts. For this reason, an elaborate procedure combining events shape and microvertex variables in a multivariate analysis is used, in order to maximize the event information and to take advantage of the high precision of the DELPHI microvertex detector. Physical quantities are extracted from the data without any explicit reference to a simulation model, in such a way that the results are almost independent of the modelling features (e.g. lifetimes, fragmentation functions, branching ratios). In this respect the Monte Carlo dependence is minimal.

The outline of this paper is as follows. In section 2, after a brief description of the DELPHI detector, we describe the selection and processing of the hadronic events. An overview of the tagging technique is presented in section 3. The fit procedure and the $\Gamma_{b\bar{b}}/\Gamma_{had}$ measurement are described in sections 4 and 5. Section 6 is devoted to the discussion of the systematic uncertainties and in section 7 appear the results and the combination with the 1991 analysis.

2 Track and Event Selection

The DELPHI detector has been described in detail elsewhere [5]. Therefore we shall mention here only the main features of the vertex detector (VD) which is essential to our analysis.

The vertex detector in the 1991/92 configuration is formed by 3 concentric shells of Si-strip detectors at radii of 6.5, 9 and 11 cm respectively. It covers the central region over a length of 24 cm and defines an angular acceptance of $27^0 - 153^0$, $37^0 - 143^0$ and $42^0 - 138^0$ for hits in one, two or three layers. Each layer is composed of 24 azimuthal modules with about 10% overlap in ϕ and each module consists of 2×4 plaquettes along z. The intrinsic $r\phi$ resolution per layer, including alignment errors, has been evaluated

to be $8\mu m$.

This analysis is based on 440k real events collected in 1992 and passing the selection cuts, which are the same as in reference [3]. For cross-checking we have used a simulated sample of 549k events generated with a b lifetime of 1.6 ps [9] after passing the same cuts.

The trajectories of charged particles include the microvertex hits. The trajectory is extrapolated to the point of closest approach to the z axis ('along the beam'), taking the traversed material into account in the error matrix. After this fit, the events are selected according to the cuts described in [3]. A cut at 0.75 was made on the cosine of the polar angle of the sphericity axis. This ensured that most of the tracks are within the acceptance of the microvertex detector.

The bias of $Z \to b\bar{b}$ fraction in the final sample is small ($0.74 \pm 0.28\%$) and has been taken into account in all presented results.

3 The tagging technique

Each event is subdivided into two hemispheres by a plane normal to the sphericity axis. The particles are distributed in jets using the LUND algorithm (LUCLUS) with $d_{join} = 2.5$ GeV and the jet direction is given by the internal thrust axis. All particles assigned to jets making an angle of less than 90^0 with the sphericity axis are attributed to hemisphere 1, the other ones to hemisphere 2. In order to improve the independence between opposite hemispheres, a primary vertex is computed on each side with an iterative procedure which includes all the charged particles in that hemisphere.

The beam spot position and dimensions were measured fill by fill. This information has been used as a constraint in the vertex fit. The measured horizontal beam spot size was around $100\mu m$ in average and the vertical one around $10\mu m$. The inclusion of this constraint increases the discriminating power of the tagging, but it represents a common feature of the hemispheres.

The tagging algorithm is based on a multidimensional analysis. The details of the technique can be found in [6] [7] and are the same that were applied for the 1991 analysis [3] [4]. Here we just mention the general features.

The probabilities p_{uds}, p_c and p_b to observe a set of tagging variables for each hemisphere of event are computed from model distributions [1]. The logarithm of these three probabilities, called *class-likelihoods* ($L_{uds} = ln\ p_{uds}$, $L_c = ln\ p_c$ and $L_b = ln\ p_b$), are the basis of our classification.

The hemispheres are first classified into 3 tags as follows (the u, d and s flavours were merged in a single uds light "tag", since the tagging variables have the same distributions for these three flavours). The flavour likelihoods are sorted in decreasing order as L_{first}, L_{second}, L_{third}. The hemisphere is tagged uds, c or b according to the highest probability L_{first}. We introduce a *winning margin*

$$\Delta = ln(p_{first}/p_{second}) \ = \ L_{first} - L_{second} \tag{1}$$

which is a sensitive indicator of tag clarity. Figure 1 represents the distributions of the *winning margin* observed in the simulation for the three tags.

[1] These model distributions are taken from a training sample of simulated events.

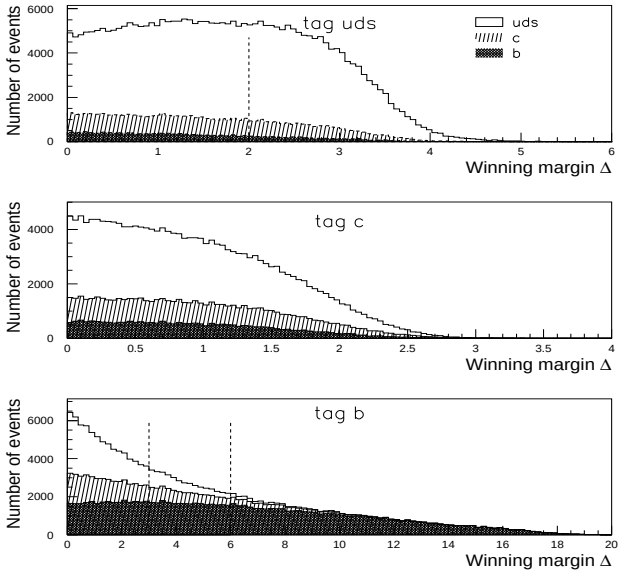

Figure 1: *Distributions obtained from Monte-Carlo of the winning margin* Δ *in the uds-tag, the c-tag and the b-tag. Each filled area style shows the different flavour contributions to the events in a given tag. The values of the cuts defining the categories are indicated.*

In order to define the six categories [3], the uds and b tags are subdivided into categories according with the following criteria:

- $uds - clear : \Delta > \Delta_{uds}^{cut}$ (category 1)
- $uds - loose : \Delta < \Delta_{uds}^{cut}$ (category 2)
- $b - loose : \Delta < \Delta_{b}^{cut,low}$ (category 4)
- $b - medium : \Delta_{b}^{cut,low} < \Delta < \Delta_{b}^{cut,up}$ (category 5)
- $b - clear : \Delta > \Delta_{b}^{cut,up}$ (category 6)

The values of the cuts are $\Delta_{uds}^{cut} = 2.0$, $\Delta_{b}^{cut,low} = 3.0$ and $\Delta_{b}^{cut,up} = 6$. They are chosen in order to have similar population in the categories. The c-tag (category 3) is less populated and poorly enriched. It has not been subdivided.

4 The fit procedure

The mathematical formalism of the fit procedure can be found in reference [3]. The tagging algorithm classifies the hadronic events into $N_T = 6$ categories, where N_T is greater than the number $N_F = 3$ of flavours.

The first set of observables is the matrix $D_{IJ}, (I, J = 1, ..., N_T)$ defined as the fraction of events tagged as I and J for hemispheres 1 and 2 respectively. The expected fraction of events T_{IJ} can be written as

$$T_{IJ} = \sum_l C_I^l C_J^l (1 + \rho_{JI}^l) R_l \tag{2}$$

In eq. (2), R_l is the flavour fraction for a given sample (R_b is the branching ratio we want to extract). C_I^l is the probability to classify an hemisphere of flavour l into the category I. The 6×3 array C_I^l (called *classification matrix*) is assumed to be the same for both hemispheres. Except for light flavours and very hard gluon emission, the quark and the antiquark are produced in opposite hemispheres, therefore the same flavour index should be associated with both hemispheres. In a first approximation, the probability to classify an event of a given flavour l in one hemisphere is independent of the classification in the other hemisphere. In order to take into account inter-hemisphere correlations a correlation matrix ρ_{JI}^l is introduced

$$\rho_{JI}^l = \frac{D_{IJ}^l}{C_I^l C_J^l} - 1 \tag{3}$$

where D_{IJ}^l is the double tag fraction for flavour l. If the hemispheres are independent, all ρ_{JI}^l elements are equal to zero. The values of these elements estimated from simulation are shown in figure 2 with their statistical errors for the six categories. Most of them are small or not significant [2].

It is not possible to extract R_b by a simple fit of the matrix D_{IJ} because of the rotation degeneracy explained in [3]. To solve this problem, a second set of observables used in the fit are the distributions of the category fractions $f_I(\delta)$. Among the events which have been tagged b in one hemisphere with a winning margin $\delta_i < \Delta < \delta_{i+1}$, let us consider the number $N_I(\delta_i)$ of events classified in the category I for the other hemisphere. The fraction $f_I(\delta_i)$ for the bin i is

$$f_I(\delta_i) = \frac{N_I(\delta_i)}{\sum_J N_J(\delta_i)} \tag{4}$$

It has been shown in ref. [3] that, if the hemispheres are independent, these distributions tend towards C_I^b when b purity is achieved in the b tag hemisphere for large values of δ. The validity of this assumption of high purity can be seen in figure 1. If one takes into account correlations between hemispheres the asymptotical value is

$$X_I^b = \lim_{\delta \to \infty} f_I(\delta) = (1 + \rho_I^{b,asym}) C_I^b \tag{5}$$

where $\rho_I^{b,asym} = \lim_{\delta \to \infty} \rho_{I6}^b(\delta)$ is the asymptotical correlation coefficient for each tag I. Monte Carlo studies [3] have shown a good stability of $\rho_{I6}^b(\delta)$ when δ increases. To a good aproximation $\rho_I^{b,asym}$ can be taken equal to $\rho_{I6}^b(6.0)$, i.e. to the element ρ_{I6}^b of the correlation matrix defined in eq. (3). Therefore, apart from the potential bias due to $\rho_I^{b,asym}$, the X_I^b asymptotes of the $f_I(\delta)$ distibutions are estimators of the C_I^b column of the classification matrix.

After a detailed study, it was found experimentally that the best parametrization of the $f_I(\delta)$ distributions for the DELPHI data is the exponential function with a gaussian resolution function,

[2] For example, the largest factor is $\rho_{11}^b = 0.52 \pm 0.15$, but it affects only $1/1000$ of $b\bar{b}$ events.

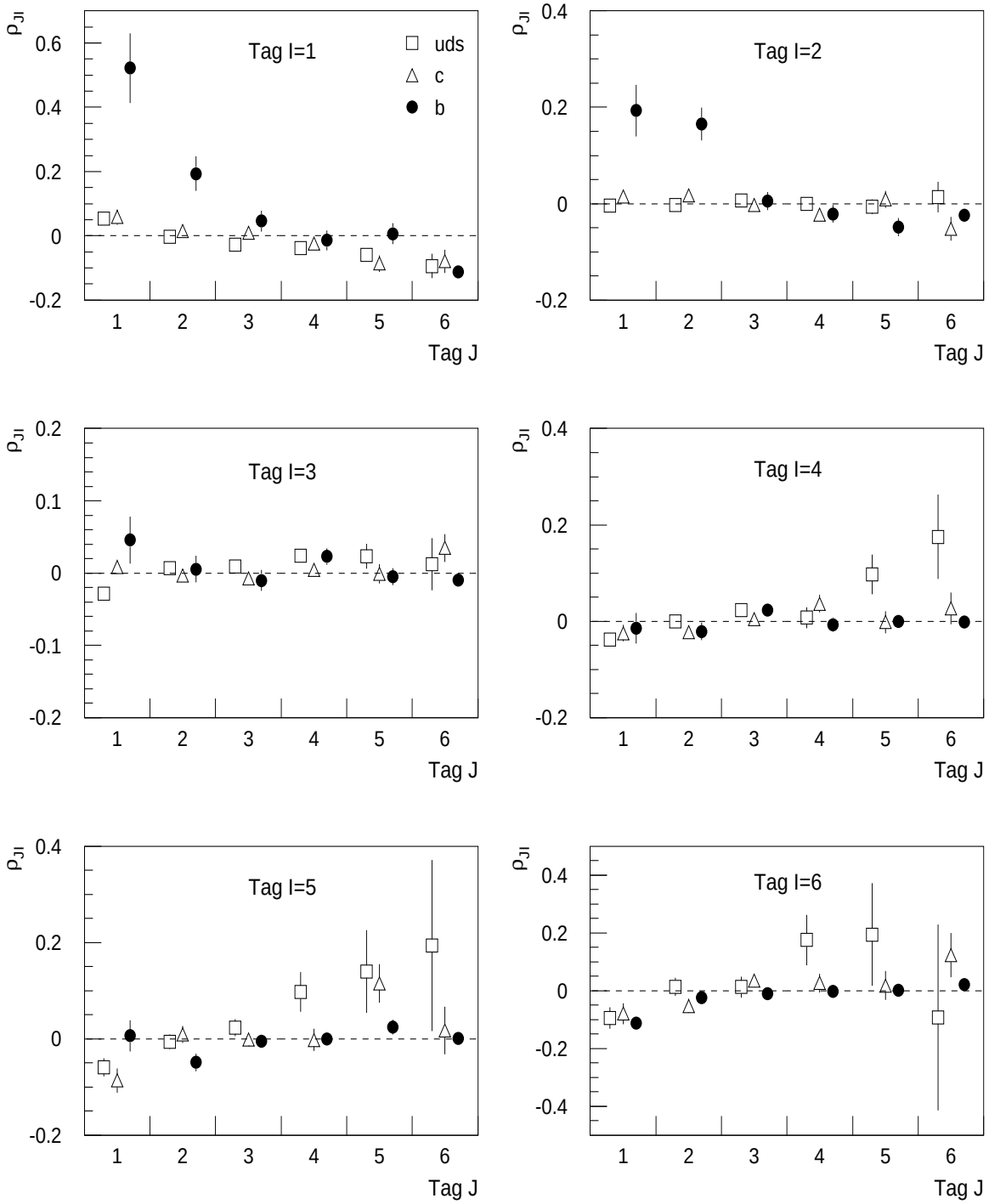

Figure 2: *Double tag hemisphere correlation factors* ρ^l_{JI}.

$$f_I(\delta) = X_I^b \ + \ f_I^{shape}(\delta) = X_I^b \ + \ \frac{a_I}{\sqrt{2\pi}c_I} e^{-b_I\delta} e^{-\delta^2/2c_I^2} \qquad (6)$$

where the a_I, b_I and c_I are free parameters. Parameters b_I and c_I give only the shape of the distribution function and a_I is a scale parameter.

For the 1991 analysis, eq. (6) was used to fit the $f_I(\delta)$ fractions to extract X_I^b. These estimators of the C_I^b column were injected in a final fit of the matrix D_{IJ} to extract R_b. For the new data we have decided to simplify this procedure, by merging the two fits into a single one. We minimize the global objective $G(C,R)$ function defined as

$$G(C,R) = \sum_{IJ} \frac{\{D_{IJ} - T_{IJ}\}^2}{\sigma_{IJ}^2} \ + \ \sum_{I,\delta} \frac{\left\{f_I(\delta) - C_I^b(1+\rho_I^{b,asym}) - f_I^{shape}(\delta)\right\}^2}{\sigma_{f_I(\delta)}^2} \qquad (7)$$

This allows the simultaneously determination of the classification matrix and the R_l compositions. The σ_{IJ} are the statistical errors of the D_{IJ} elements and the $\sigma_{f_I(\delta)}$ is the experimental error on $f_I(\delta)$ for each bin of δ. With this function, a remaining degeneracy in the $uds-c$ sector is still present but it can be removed for instance by fixing R_c to the standard model value or to the current measured value. It should be remarked that this constraint has no effect on any parameter of the b sector.

The fit solution has to be compatible with the following constraints:

- $\sum_I C_I^l = 1$ for all values of l;
- $\sum_l R_l = 1$;
- $\sum_{IJ} D_{IJ}^l = \sum_{IJ} C_I^l C_J^l (1+\rho_{JI}^l) = 1$ for all values of l; and
- $\sum_I C_I^b (1+\rho_I^{b,asym}) = 1$.

The method of Lagrange Multipliers is appropriate to deal with this problem. The matrix itself has to obey the normalization condition $\sum_{IJ} D_{IJ} = 1$ with the requirement of symmetry $D_{IJ} = D_{JI}$. With the 6 categories, the binning of $f_I(\delta)$ and assuming that the ρ_{JI}^l are zero, the total number of independent observables is 220 for 35 independent parameters to fit [3].

The advantages of this global fit are mainly two: first, correlation effects (matricial and asymptotical ones) can be studied simultaneously with the two sets of observables; second, the final solution is the best compatible between the set of degenerated solutions (given by the first term of the G function) and the estimates of the b tagging efficiencies (second term of G).

Some events, in particular of the b flavour, enter in the term D_{IJ} and in the distributions $f_I(\delta)$. The definition of the $G(C,R)$ function does not take into account this "double counting". In order to estimate correctly the statistical error, we have generated artificial data sets by fluctuating randomly the number of events on the cells of the matrix D_{IJ} and on the bins of the distributions $f_I(\delta)$ by considering their correlation. The dispersion of the fitted R_b was taken as the statistical error of the fit. This error agrees within 5%

[3] When all ρ_{JI}^l are taken zero the constraints $\sum_{IJ} D_{IJ}^l = 1$ and $\sum_I C_I^b(1+\rho_I^{b,asym}) = 1$ are the same as $\sum_I C_I^l = 1$. Therefore, by considering correlations the total number of degrees of freedom increases to 189.

with the estimation given by the $\chi^2 + 1$ method and therefore we conclude that the net effect of this "double counting" is small. [4]

5 $\Gamma_{b\bar{b}}/\Gamma_{had}$ measurement

5.1 Monte Carlo cross-checking

We have minimized the function $G(C, R)$ with the Monte Carlo sample, fixing the R_c parameter to the "world" measured value of 0.171 [10]. As has already been remarked, this constraint has no effect on any parameter of the b sector. Figure 3 shows the population of the double tagged categories. The contributions of the three flavours are detailed also there. As can be seen uds and b events populate opposite corners, while c events overlap largely with uds and b. The plots of the $f_I(\delta)$ distributions as a function of the clear winning cut value δ with the results of the fit are shown in figure 4. The validity of the assumption of the asymptotic fit that there is no irreducible background from light and c quarks can be clearly seen in the figure.

Figure 5 compares the C_I^b fitted values when one take all correlation coefficients equal to zero and when they are assigned their true values. As expected, the C_I^b fitted values using the actual correlation coefficients are neare to the corresponding true C_I^b. However, the difference with respect to the case when all correlation coefficients are taken as zero is small.

The fitted b fraction when all correlations are taken to be zero is $R_b = 0.2169 \pm 0.0036(stat)$ with $G_{min}/ndof = 218.6/185$. If one takes into account the correlations, this value change to 0.2162 with $G_{min}/ndof = 196.8/189$. These two values should be compared to the generated value of 0.217. Those results mean that only a drop of -0.0007 is found on the final fitted R_b when correlations are considered. This suggest that the sensitivity of the method to the provided pattern of correlations is small.

5.2 Real data

If one repeats the fit for the real data, asuming no correlations, the fitted b fraction is $R_b = 0.2166 \pm 0.0058(stat)$ with $G_{min}/ndof = 190.5/185$. The plots of the $f_I(\delta)$ distributions with the results of the fit are shown in figure 6. The fitted classification matrix can be seen in figure 5. The b tag efficiency in the category 6 (clear b tags) is smaller in data than on Monte Carlo. The larger statistical error of R_b on data than on simulation reflects the smaller efficiency of the tagging.

[4] A total of 50 data sets was generated. The "b" cells of the tensor D_{IJ} with I or J > 3 and the $f_I(\delta)$ were computed from the $N_I(\delta_i)$ which are the elementary obervables that were fluctuated randomly. The $non-b$ cells with I and J < 3 were fluctuated independently. This procedure takes into account exactly the double counting.

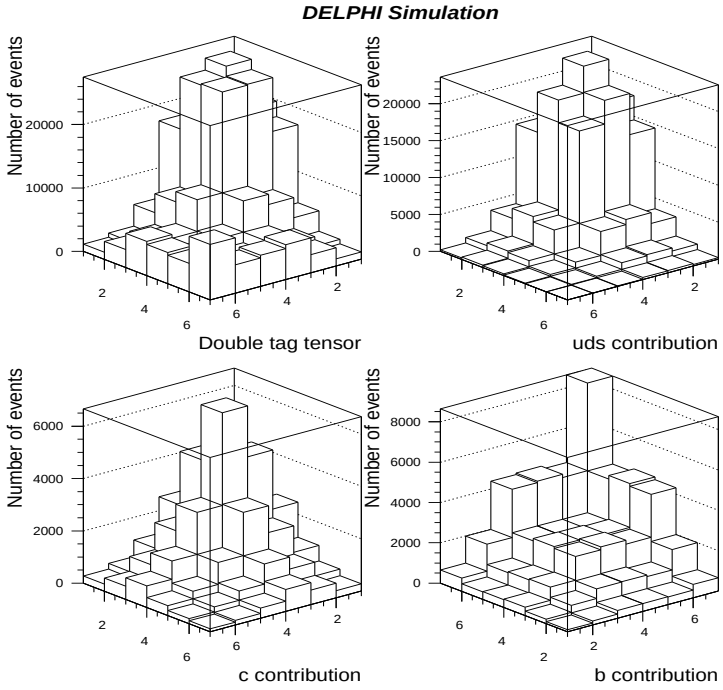

Figure 3: *Population of the double tag matrix on Monte Carlo with the uds, c and b contributions. Note that the axes for the b contribution are rotated by 180 degrees with respect to the other plots.*

6 Discussion of systematic errors

In the study of the systematic errors we have distinguished two kind of errors: errors specific to the method and errors due to uncertainties on physical parameters (non specific errors). In the latter we have followed the prescriptions of the LEP Electroweak Working Group [12] and they have been sorted in three parts: the b sector, the $uds - c$ sector and finally the influence of $\Gamma_{c\bar{c}}$. Table 1 summarizes all the contributions to the systematic error.

6.1 Specific errors to the method

6.1.1 Effect of hemisphere correlations

On Monte Carlo, a small difference on R_b (-0.0007, i.e 0.3% in relative value) is observed if one takes into account the true correlation matrix in the fit or if one neglects it. This small bias is a proof that the method is almost insensitive to the particular pattern of correlations. There is no evidence for a fundamentally different correlation pattern in real data with respect to the simulation. The error made on data in neglecting the correlation pattern should be similar to the one made on Monte Carlo. We obtain a estimate of this

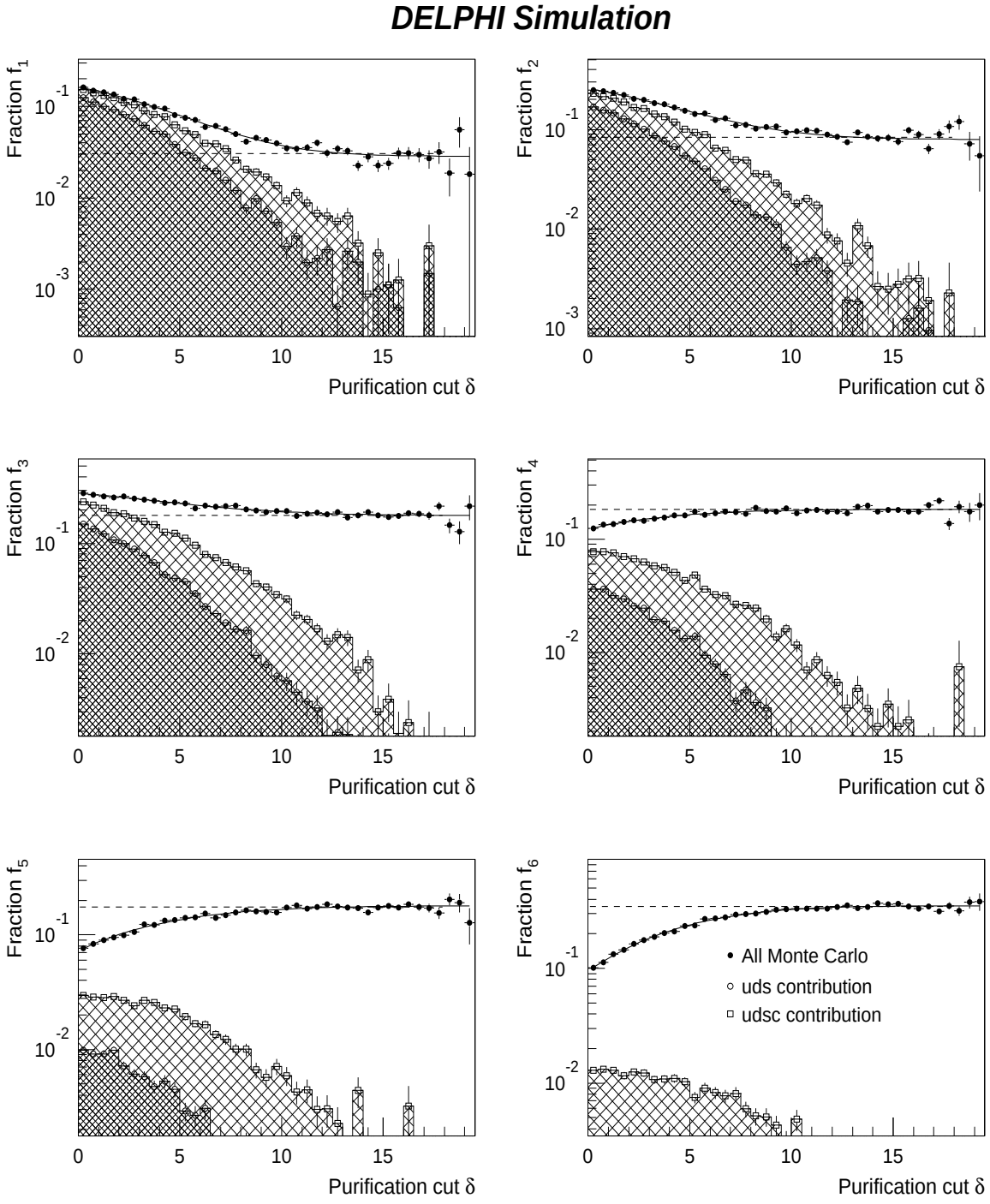

Figure 4: *$f_I(\delta)$ distributions with the results of the fit for simulation. The big cross-hatched area indicates the sum of the uds and c contaminations while the small cross-hatched area is the uds contribution. No irreducible uds and c background is observed in the asymptotic region, especially in $f_4(\delta)$, $f_5(\delta)$ and $f_6(\delta)$ distributions which are the most significant for the R_b extraction. The dotted horizontal lines show the expected C_I^b values.*

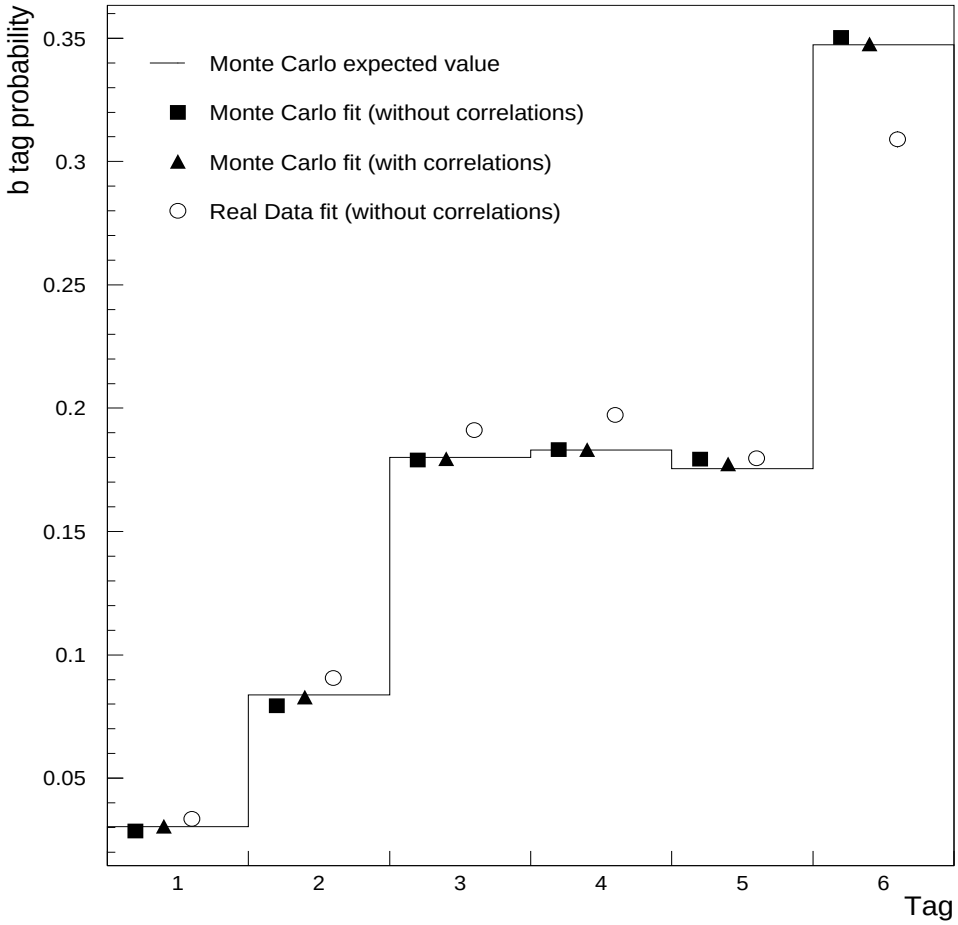

Figure 5: *Comparison between the C_I^b fitted values taking all correlation coefficients equal to zero, taking their values from simulation, and the expected values for the Monte Carlo data set. The C_I^b fitted values for the real data set are also shown. Errors are at the level of the point size.*

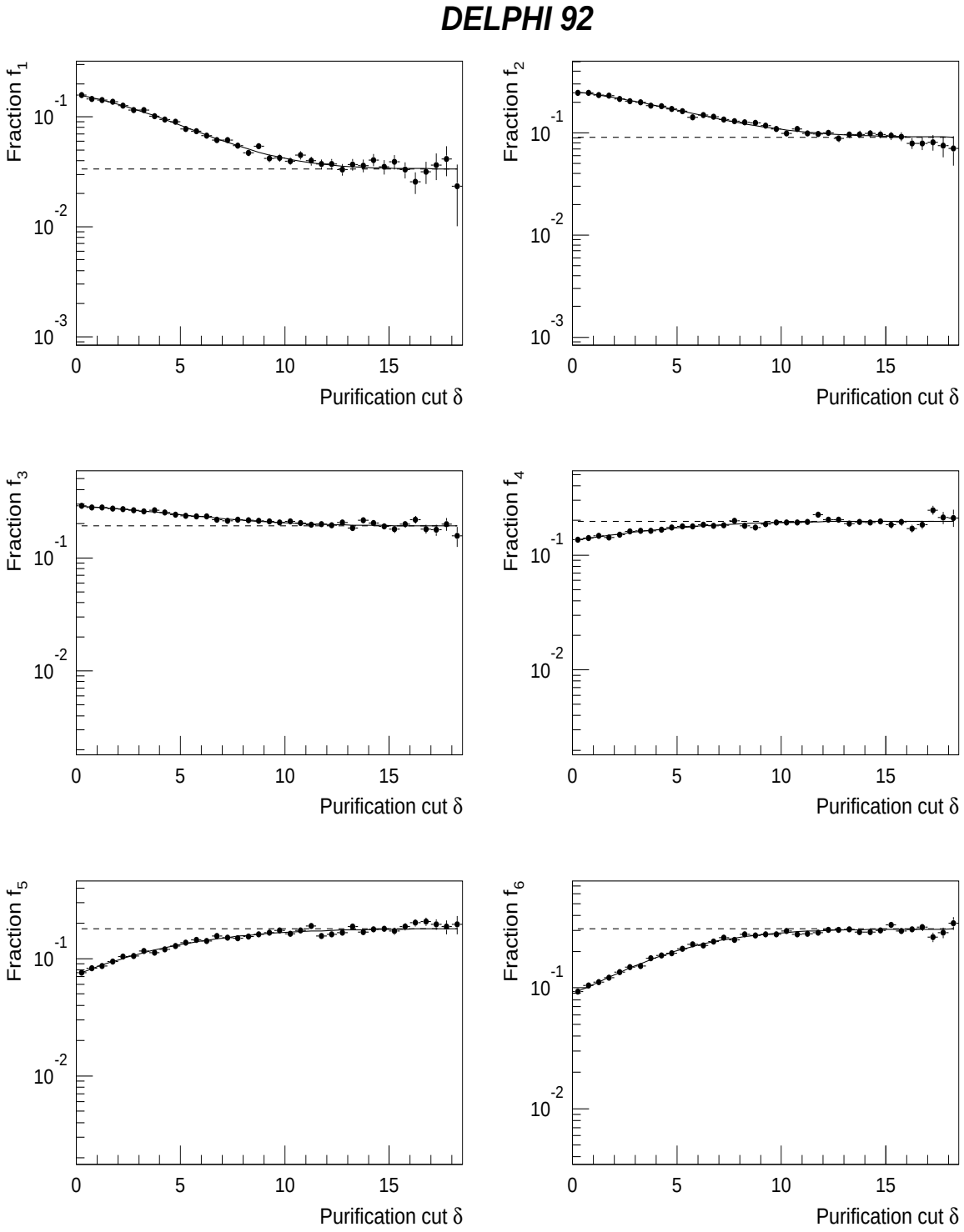

Figure 6: *$f_I(\delta)$ distributions with their asymptotic fits for DELPHI 92 real data. The dotted horizontal lines show the fitted C_I^b values.*

error by varying the ρ^l_{JI} elements around their values according to their statistical errors and by repeating the fit. We have found a dispersion on R_b of 0.0022, three times larger than the observed bias. We shall take this dispersion as the uncertainty due to the limited Monte Carlo statistics. This will be the main source of systematic error. Moreover we add the effect of individuals sources of correlation [5].

6.1.2 Effect of hard gluon emission

The effect of hard gluon emission producing a $b\bar{b}$ pair in the same hemisphere (about 2 % of the $b\bar{b}$ events according to the simulation) might be the source of an excess of b events in the *(small I,large J)* and *(large I,small J)* cells. In order to evaluate systematic errors, we have performed a fit on simulation, removing the events with two b jets in the same hemisphere and recomputing the b fraction in the reduced sample. We take for the systematic error due to this effect a 20% of the difference between the fitted value of R_b (for the sample without events with a hard gluon) and the expected one and it becomes 0.0007. 20% is deduced from the uncertainty in α_s and from the difference in the prediction of the Lund parton shower and matrix element model.

6.1.3 QCD effects

Hadronic Z events with a three or more jet topology may introduce kinematic correlations. The dependence of the R_b result upon the number of jets found in each events was examined using the Monte Carlo sample. As a cross-check the events were divided into two categories: events with two and events with three or more jets. The fit was able to follow accurately the b fractions which vary with jet multiplicity. The systematic effect was estimated by changing the expected fraction of events with a two jet topology by 20 %.

6.1.4 Errors due to apparatus

- Acceptance. The change in the b fraction due to the acceptance cuts was found to be $(0.74 \pm 0.28\%)$ from Monte Carlo simulation. This induces a systematic uncertainty on R_b of 0.0006.

- θ_{sph} correlation. Correlation could be induced due to the drop of tag efficiency at the fringes of the vertex detector acceptance. The VD acceptance cut on $\mid cos\theta_{sph} \mid$ was moved from 0.65 to 0.85 and the variation of R_b was small and consistent with the statistical fluctuations.

- ϕ_{sph} correlation. During the 1992 running, one row of the DELPHI vertex detector in one layer was dead. This tagging is not very sensitive to local defects, so the variation of the tag efficiency with the azimuthal direction ϕ_{sph} of the event axis is

[5] Asymptotic correlation factors $\rho_I^{b,asym}$ were also changed, taking into account the small instabilities of $\rho^b_{I6}(\delta)$ for running δ. A negliglible change, with respect to the previous error, was found on the final fitted R_b value.

not important. Nevertheless, we have investigated the error due to the local drop of efficiency which induce a small negative correlation and a contribution of 0.0011 was found.

6.1.5 Other specific errors

- Beam spot constraint. This constraint can be a source of correlations owing to the beam spot size, since the beam spot constraint is common for both hemispheres. A 10% uncertainty was assumed (which corresponds to the accuracy of the size determination) and a variation on R_b of 0.0004 was found.

- Effect of classification. We have taken a different training sample than the one used in the computation of the *class-likelihoods*, which are the basis of the tagging (the two training samples had different lifetimes 1.2 and 1.6 ps). Another effect to be considered is the choice of $\Delta_b^{cut,low}$ and $\Delta_b^{cut,up}$ which define the boundaries of b categories. Considering all these effects a contribution to the systematic error of 0.0007 is found.

- Fit procedure, including the choice of the $f_I(\delta)$ parametrization and bin range of the $f_I(\delta)$ distributions used in the minimization of $G(C,R)$. A remarkable stability on the fitted R_b was obtained, consistent with the statistical differences. Moreover different equivalent parametrizations of the $f_I(\delta)$ distributions (uniform in the last bins, exponential inverse polynomial functions, etc) were tried and a very good stability was obtained compatible with the small statistical differences.

6.2 Uncertainties in the b sector

In the absence of hemisphere correlations, the R_b measurement is mathematically independent of the factors that affect b production or decays, for example fragmentation or lifetimes. The fit does not use external values of the efficiencies (classification matrix) - which are sensitive to these parameters - but measures them also on the data. In the presence of non-zero correlations, a variation of these parameters may affect slightly the result of R_b. Therefore, we have checked the effect of a variation of correlation effects with the b lifetime, using the same simulated sample with different weightings. The change on R_b was 0.0006 when going from 1.6 ps to 1.2 ps. If one takes into account that the current uncertainty on the b lifetime is 0.033 ps [9], this leads to an actual contribution smaller than 0.0001. The uncertainty due to the fragmentation function was estimated by varing the mean energy of B hadrons within the error limits $< x_E(b) >= 0.70 \pm 0.02$ [12].

6.3 Errors from the charm and light quark sectors

Most methods of extraction of the R_b quantity assume the knowledge of the tag efficiencies for the uds and c flavours. These efficiencies, taken from simulation, are sensitive to theoretical uncertainties in the uds and c sectors. They are source of systematic errors.

In this method, R_b is extracted independently of these efficiencies (which are simultaneously obtained by fitting the data). In the absence of hemisphere correlations, the corresponding systematic errors are exactly zero. However, we have checked that these errors are of second order. Finally, we conservatively added these contributions in.

The uncertainty due to the fragmentation function was estimated by varing the mean energy of D hadrons within the error limits $< x_E(c) >= 0.51 \pm 0.02$ [12]. The uncertainties from the relative production rate of D hadrons, their lifetimes, decay multiplicities and inclusive branching ratios $D \to K^0 X$ were obtained by varing their measured values according to [12]. The systematic error from uncertainties in production of long lived particles in light quark events (K^0, Λ, hyperons) was obtained by variation of the corresponding production rates in simulation by $\pm$ 10%. The variation on the measured R_b was negligible. The systematics from the gluon splitting $g \to b\bar{b}$ and $g \to c\bar{c}$ was obtained from the variation of fraction of such events by 50 % as proposed in [12] and also a negligible contribution was obtained.

6.4 Error from $\Gamma_{c\bar{c}}$

The error on R_b due to actual amount of charm events (which should be distinguished from the formal R_c parameter of the fit) was estimated changing the $c\bar{c}$ fraction by one standard deviation from its measured value ($R_c = 0.171 \pm 0.014$ [10]). A variation of ∓ 0.0005 was found on the difference between the fitted and the expected values.

7 Results and combination with the 1991 analysis

A new measurement of $\Gamma_{b\bar{b}}/\Gamma_{had}$ was performed using a multidimensional analysis technique. The tagging uses the high precision tracking information given by the DELPHI microvertex detector. With the double hemisphere tagging and with a simultaneous fit of the double tag matrix and the b winning margin distributions, the tagging efficiencies and the ratio $\Gamma_{b\bar{b}}/\Gamma_{had}$ are directly obtained by fitting the data, without any explicit reference to a simulation model, in such a way that the results are almost independent of the modelling features. In this respect the Monte Carlo dependence is minimal. The quoted value of $\Gamma_{b\bar{b}}/\Gamma_{had}$ for 1992 data from about 440000 hadronic Z decays is

$$\Gamma_{b\bar{b}}/\Gamma_{had} = 0.2166 \pm 0.0058(stat) \pm 0.0031(syst) \pm 0.0005(\Gamma_{c\bar{c}} syst)$$

where the main contribution to the systematic error is due to the limited Monte Carlo statistics.

In order to combine the analysis presented here with a similar one made with the 1991 data, the following assumptions are made:

- All statistical errors are assumed to be independent.
- The errors due to QCD effects and hard gluon emission are taken fully correlated.
- The error from acceptance bias was assumed uncorrelated. All the other specific errors to the method are taken fully correlated.

- The uncertainties due to the b fragmentation and b lifetime are assumed to be fully correlated.
- The errors from the charm and light quark sectors are also taken as fully correlated.
- The error due to $\Gamma_{c\bar{c}}$ was assumed to be fully correlated.

With these assumptions the combined result is

$$\Gamma_{b\bar{b}}/\Gamma_{had} = 0.2196 \pm 0.0044(stat) \pm 0.0029(syst) \pm 0.0005(\Gamma_{c\bar{c}} syst)$$

Table 1 summarizes all the contributions to the systematic error for the current analysis and for the combined result.

Source	Range of variation	σ_{syst} (1992)	σ_{syst} (1991+1992)
Monte Carlo statistics		0.0022	0.0022
Acceptance bias		0.0006	0.0005
Azimuthal angle acceptance		0.0011	0.0007
Beam spot size	$\pm 10\%$		0.0004
Effect of tagging		0.0007	0.0009
Effect of hard gluon emission	See text		0.0007
QCD effects	See text		0.0009
b quark fragmentation	$< x_E(b) >= 0.70 \pm 0.02$		0.0004
Average b lifetime	1.538 ± 0.033 ps		0.0001
c quark fragmentation	$< x_E(c) >= 0.51 \pm 0.02$		0.0003
D decay multiplicity	2.39 ± 0.14		0.0003
$Br(D \to K^0 X)$	0.46 ± 0.06		0.0004
D^0 fraction in $c\bar{c}$ events	0.557 ± 0.053		0.0005
D^+ fraction in $c\bar{c}$ events	0.248 ± 0.037		0.0003
D_s fraction in $c\bar{c}$ events	0.12 ± 0.05		0.0007
D^0 lifetime	0.420 ± 0.008 ps		0.0001
D^+ lifetime	1.066 ± 0.023 ps		0.0002
D_s lifetime	0.450 ± 0.0030 ps		0.0001
Λ_c lifetime	0.191 ± 0.0015 ps		0.0002
Production of light hadrons	Tuned JETSET $\pm 10\%$		0
Gluon splitting	See text		0
$c\bar{c}$ events ($\Gamma_{c\bar{c}}/\Gamma_{had}$)	0.171 ± 0.014		0.0005
Total systematic error		0.0032	0.0030

Table 1: *Contributions to the systematic error on $\Gamma_{b\bar{b}}/\Gamma_{had}$ for the 1992 analysis and the obtained one from the combination with the 1991 result. The values which are the same in the combined result than in the 1992 analysis are only writen for the combined one.*

The measured $\Gamma_{b\bar{b}}/\Gamma_{had}$ value is in good agreement with the Standard Model prediction computed with the ZFITTER program [11] and with previously published measurements [8]. The weak dependence of $\Gamma_{b\bar{b}}/\Gamma_{had}$ on $\Gamma_{c\bar{c}}/\Gamma_{had}$ avoids important systematic uncertainties from the charm sector.

Acknowledgements

We are greatly indebted to our technical collaborators and to the funding agencies for their support in building and operating the DELPHI detector, and to the members of the CERN-SL Division for the excellent performance of the LEP collider.

References

[1] J.H. Kühn, P.M. Zerwas in 'Z physics at LEP 1', Ed. G. Altarelli et al., CERN TH/89-08 (1989), Vol. 1, p. 271.

[2] J. Bernabeu, A. Pich, A. Santamaria, Phys. Lett. B200 (1988) 569.
B. W. Lynn and R. G. Stuart, Phys. Lett. B252 (1990) 676.
M. Boulware, D. Finnell, Phys. Rev. D44 7 (1991) 2054.
J. Bernabeu, A. Pich, A. Santamaria, Nucl. Phys. B363 (1991) 326.

[3] P. Billoir *et al.* 'Measurement of the $\Gamma_{b\bar{b}}/\Gamma_{had}$ branching ratio of the Z by Hemisphere double tagging with minimal Monte Carlo dependence'. DELPHI 93-137 PHYS 347 (1993).

[4] P.Abreu *et al.* (DELPHI Collaboration), 'Measurement of the $\Gamma_{b\bar{b}}/\Gamma_{had}$ Branching Ratio of the Z by Double Hemisphere Tagging', CERN-PPE, 1994, preprint in preparation and contribution to this Conference.

[5] P. Aarnio *et al.* (DELPHI Collaboration). NIM A 303 (1991) 233.

[6] Ch de la Vaissiere, S. Palma-Lopes. 'Multidimensional Analysis: A Tool for B-Tagging ?' DELPHI 89-32 PHYS 38. 1989.

[7] P. Billoir *et al.* 'B-tagging by hemisphere: description of variables and results on Monte Carlo'. DELPHI 93-54 PHYS 282. 1993.

[8] D. Buskulic *et al.* (ALEPH Collaboration), CERN-PPE/93-108, 1993.
D. Buskulic *et al.* (ALEPH Collaboration), CERN-PPE/93-113, 1993.

[9] S. Squarcia, 'Heavy Flavour Physics at LEP', CERN-PPE/94-69, 1994.

[10] The LEP Collaborations, 'Updated Parameters of the Z^0 Resonance from Combined Preliminary Data of the LEP Experiments ', CERN-PPE/93-157, 1993.

[11] D. Bardin *et al.*, 'ZFITTER: An Analytical Program for Fermion Pair Production in e^+e^- Annihilation', CERN-TH, 6443/92.

[12] The LEP Electroweak Working Group, ALEPH note 94-90, DELPHI 94-23/add, L3 note 1613, OPAL technical note TN237, 10 June 1994.